Molecular investigation to quantify the translocation of siRNA-NAPA oligomer complexes through lipid membrane

Desh Deepak Yadav,[a] Debdip Bhandary,[b,*] and Pradip Paik[a,†]
[a]*School of Biomedical Engineering*, and [b]*Department of Chemical Engineering & Technology, Indian Institute of Technology (BHU) Varanasi, Uttar Pradesh – 221005, India*
Corresponding authors: **debdip.che@iitbhu.ac.in; †paik.bme@iitbhu.ac.in*

Model and Methodology

The symmetric POPC lipid membrane model consists of 330 lipids in both upper and lower leaflets, spanning the simulation box on the x-y plane (14 nm × 14 nm), with a surface density of 0.65 nm^2/molecule, constructed and solvated in water using the CHARMM-GUI membrane builder.[1] The naked-siRNA/siRNA-NAPA oligomer complexes(Fig.S1) were taken from our previous work.[2] Interactions between atoms in all atomistic models were set up using the CHARMM36 force field. The center of mass of either naked-siRNA or siRNA-NAPA oligomer complex was placed at a distance of 5 nm from the lipid bilayer's center of mass, i.e., center of mass of all of the lipid molecules without any specific orientational preference, and was solvated subsequently. Solvation was performed using the TIP3P water model, and an appropriate number of sodium and chloride ions were added to neutralize the system. All simulations were conducted using GROMACS 2020.2[3], with periodic boundary conditions in all three dimensions. The solvated system was subjected to energy minimization using the steepest descent algorithm with a convergence criterion of 1000 $kJ \cdot mol^{-1} \cdot nm^{-1}$, which removed any non-physical contacts between the molecules. To integrate the equation of motion, the Leap-frog algorithm was used with a timestep of 2 fs. PME was used to compute the long-range electrostatic interactions with a real-space cutoff distance of 12 Å.[4] The vdW interaction was truncated at a distance of 12 Å. These minimized structures were heated to 300 K in an NVT ensemble using a velocity rescaling thermostat, with a coupling time of 0.1 ps. Thermally equilibrated systems were further relaxed to equilibrate at a constant pressure of 1 atm and a temperature of 300 K, using the Parrinello-Rahman barostat (coupling time constant of 2 ps) and the velocity rescaling thermostat (coupling time constant of 0.1 ps), respectively. The POPC membrane was pressure-coupled, semi-isotropic, allowing it to move in the x-y plane independently of the z-axis. A one-nanosecond additional equilibration run was performed under the NpT ensemble without restraining the system.

Excess entropy (S_{excess}) is calculated using the radial distribution function, $g(r)$, obtained via the two-particle correlation between the phosphate atoms in the upper-leaflet of the POPC membrane.[5] It is expressed as:

$$S_{\text{excess}} \approx -2\pi\rho k_B \int_0^{\infty} \big(g(r)\ln g(r) - g(r) + 1\big) r^2 dr. \tag{1}$$

The radial distribution function was calculated over the last 200 ps of each 2 ns, using particle positions at every 2 ps. The integral was computed using the trapezoidal rule, which is second-order accurate, with an error of $O(\Delta r^2)$.

Mean curvature (H) is the average bending at each point on the membrane. We have calculated the mean curvature for the upper leaflet phosphate atoms for local curvature quantification using the Monge patch[6] with every 1 picosecond sampling frequency :

$$H = \frac{1}{2} \frac{\big(1+h_y^2\big) h_{xx} - 2h_x h_y h_{xy} + \big(1+h_x^2\big) h_{yy}}{\big(1+h_x^2+h_y^2\big)^{3/2}}, \tag{2}$$

where h_x, h_y are the first derivatives of the height field and h_{xx}, h_{yy}, h_{xy} are their second derivatives represents local bending.

Enhanced Sampling Technique:

Steered molecular dynamics (SMD) simulations were conducted to generate the initial configurations for umbrella sampling (US) simulations by pulling the center of mass of siRNA/siRNA-NAPA oligomer complex along the reaction coordinate (along the z-axis), producing a series of snapshots at incremental positions that serve as the starting configurations for the US windows. A high pulling velocity of 10 m/s was applied to drive the naked siRNA and the corresponding polyplexes across the membrane. This ensures that the naked siRNA and the polyplexes experience pulling forces in the aqueous

phase, enabling them to surmount the free-energy barrier at the membrane interface. Umbrella sampling, an enhanced sampling technique, is often used to estimate the free energy. A series of equi-spaced configurations was extracted from the trajectories of SMD simulations. A harmonic potential having a force constant of 1000 kJ $mol^{-1}nm^{-2}$ was applied to restrain the distance (i.e., reaction coordinate, ξ) between the center of mass of the lipid bilayer and that of siRNA-NAPA oligomer complexes. For different polyplexes, 35 different configurations were considered, with a change in ξ of 2 Å. The windows were first equilibrated for 1 ns in an NpT ensemble (simulation parameters mentioned above) and subsequently allowed to evolve for 5 ns (see Fig.S7). The simulation outcomes were analyzed using the weighted histogram analysis method (WHAM) to estimate the free energy profile of the naked-siRNA/siRNA-NAPA oligomer complexes relative to the lipid bilayer as a function of the reaction coordinate (ξ).

Results and Discussions

Molecular structures of siRNA, siRNA-NAPA oligomer complexes, and NAPA oligomers

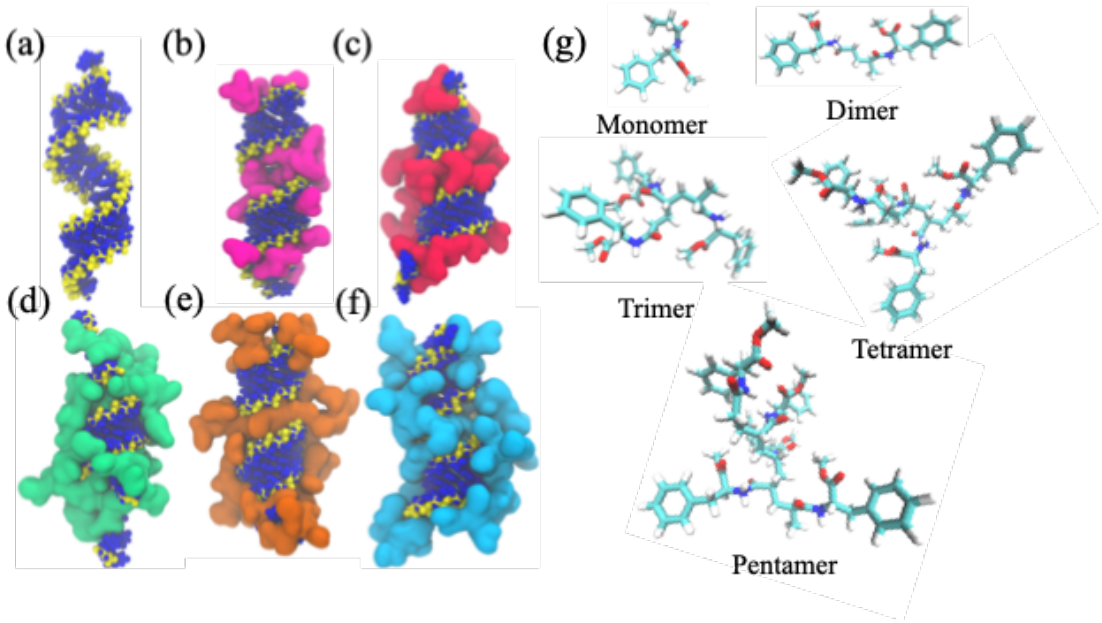

Fig. S1 Snapshot of the initial structure of siRNA (a) and siRNA–NAPA oligomer complexes (b-f), where NAPA oligomers, shown in different colours (colour code is the same as in Figure 1), are within the groove spacing of siRNA strands. (b–f) show polyplexes—monomer, dimer, trimer, tetramer, and pentamer, respectively. (g) shows the molecular structures of the NAPA oligomers (monomer-pentamer) where carbon, hydrogen, nitrogen, and oxygen atoms are shown in cyan, white, blue, and red colors, respectively.

Fig.S1 illustrates the molecular arrangement of siRNA and the siRNA–NAPA oligomer complex (polyplex), where the NAPA oligomers occupied the grooves formed by the siRNA strands and attained stable structures. The siRNA–NAPA interaction is dominated by electrostatic attraction between protonated amines(NH_2) on NAPA and the phosphate backbone of siRNA, further stabilized by extensive hydrogen bonding(NAPA amines with phosphate oxygens of siRNA) and water-mediated contacts (water bridging NAPA amines and phosphate oxygens) within the grooves. Through electrostatic interactions, the oligomers wrap around and compact the siRNA molecule, significantly reducing its hydrodynamic size while largely preserving its native A-form helical conformation. This structural preservation is critical for maintaining siRNA biological activity. Additionally, this complexation effectively shields the siRNA from enzymatic degradation, while the terminal ends are accessible and free for chemical modification.[2]

Dynamics of siRNA and polyplexes near the lipid bilayer

Fig.S2 shows the snapshot of siRNA and polyplexes near the POPC membrane, illustrating the dynamic behavior of siRNA and polyplexes in proximity to a lipid membrane. The initial configurations of the systems (at $t = 0$ ns) for both siRNA

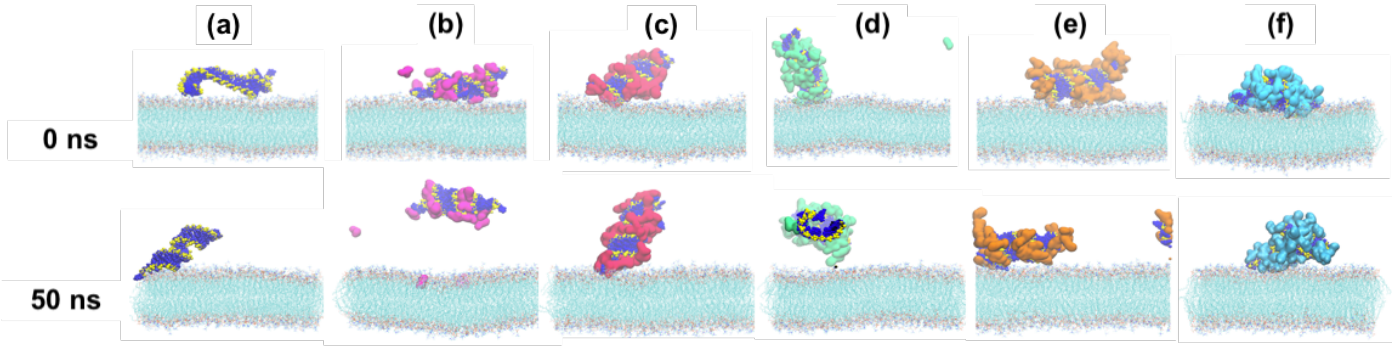

Fig. S2 Snapshots of siRNA and polyplexes in the vicinity of the POPC membrane. The top panels of (a-f) show the molecular structure at t=0 ns, while the bottom panels depict the intermediate configurations of respective systems at t=50 ns. Colour code is the same as in Figure 1.

and polyplexes were deliberately positioned near the lipid membrane to reduce computational expense. Intermediate configurations ($t = 50$ ns) of each system are subsequently displayed, revealing significant conformational and positional changes over the course of the simulation. At this stage, a notable heterogeneity in monomer behavior is observed (Fig.S2(b)) — a few monomer molecules are found to be either impregnated into the lipid membrane bilayer or diffusing in the surrounding aqueous solution, while the remaining molecules maintain a stable complex with the siRNA, highlighting the dynamic nature of this polyplex.

Temporal evolution of polyplexes and lipid bilayer

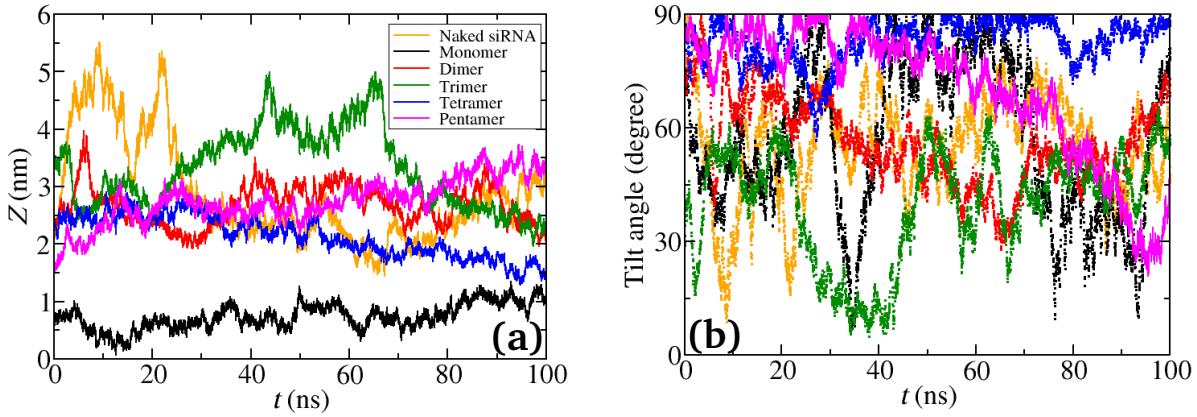

Fig. S3 Temporal evolution of (a) distance between the center of mass of siRNA/polyplexes and the center of mass of phosphorus atoms of the upper leaflet and (b) tilt angle between the siRNA and membrane normal over the trajectory.

Fig.S3(a) illustrates the temporal variation in the distance between the center of mass of siRNA and the center of mass of phosphorus atoms residing in the upper leaflet of the lipid membrane, monitored continuously throughout the 100 ns unbiased molecular dynamics trajectories across various simulated systems. At the onset of the simulations, both siRNA and polyplexes are positioned away from the membrane surface. As the simulations progress, the distances exhibit fluctuations; however, these variations remain negligible over the entire 100 ns simulation period. This observation indicates that, although the polyplexes reside in close proximity to the membrane surface, they are unable to spontaneously translocate across the lipid bilayer within the simulated timescale. This inability to translocate underscores the inherent energetic barriers to membrane crossing, thereby underscoring the need to employ enhanced sampling techniques to capture and study the complete translocation mechanism of siRNA and its carrier complexes.

Polyplexes translocation

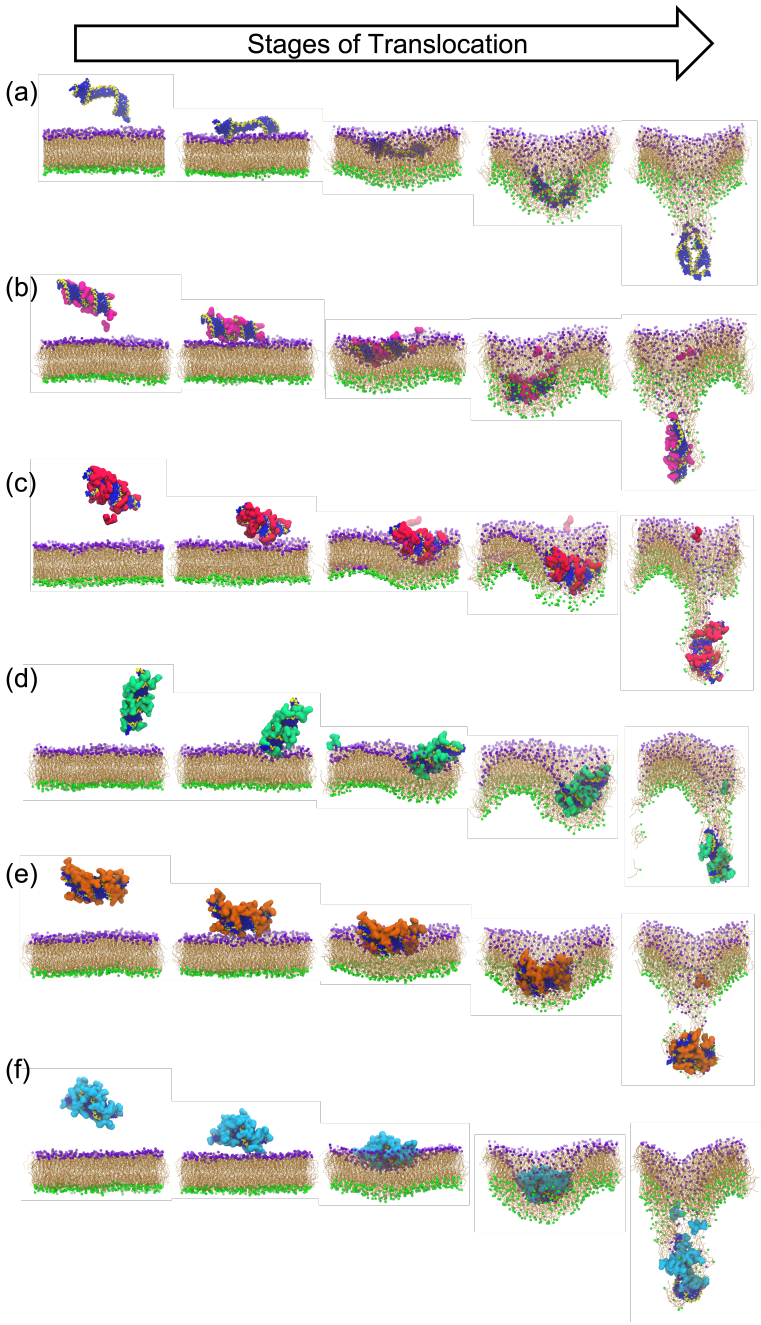

Fig. S4 Simulation snapshots capturing (a) siRNA and (b-f) polyplexes (arranged top to bottom) at different stages of membrane translocation (left to right in every row) during SMD simulations. Color code: as in Figure 1.

Fig.S4 displays the Steered Molecular Dynamics (SMD) configurations for all simulated systems through a series of representative snapshots that collectively demonstrate the gradual and stepwise internalization process of (a) siRNA and (b-f) polyplexes across the POPC lipid bilayer membrane, progressing chronologically from left to right. At the initial stage, depicted in the leftmost panels, both naked siRNA and its respective polyplexes are uniformly distributed in the aqueous phase, approximately 5 nm from the membrane surface, representing the pre-insertion state prior to any membrane interaction. In the intermediate snapshots, naked siRNA and polyplexes are observed migrating toward the membrane, progressively establishing meaningful contacts with the headgroup components of the upper leaflet, specifically interacting with the phosphate and choline groups that constitute the outer membrane interface. These interactions mark

the beginning of the membrane engagement phase, in which electrostatic and hydrophobic forces drive the complexes toward deeper membrane penetration. Finally, the concluding snapshots in the rightmost panels demonstrate complete translocation of both naked siRNA and polyplexes to the lower leaflet of the bilayer, accompanied by pronounced, visually significant membrane buckling along the pulling direction, reflecting the substantial mechanical deformation induced during forced translocation. A particularly notable and striking observation throughout the SMD pulling simulations is the distinct orientational transformation undergone by naked siRNA and polyplexes during intermediate phases. In the middle snapshots, the complexes adopt characteristic submarine configurations, orienting themselves perpendicular to the membrane normal as they engage with the bilayer. However, as the pulling force draws the complexes further toward the lower leaflet, this submarine configuration dynamically transitions into a rocket configuration, wherein the siRNA and polyplexes realign parallel to the membrane normal, facilitating their ultimate passage through the lipid bilayer.

Conformational dynamics and orientations of polyplexes

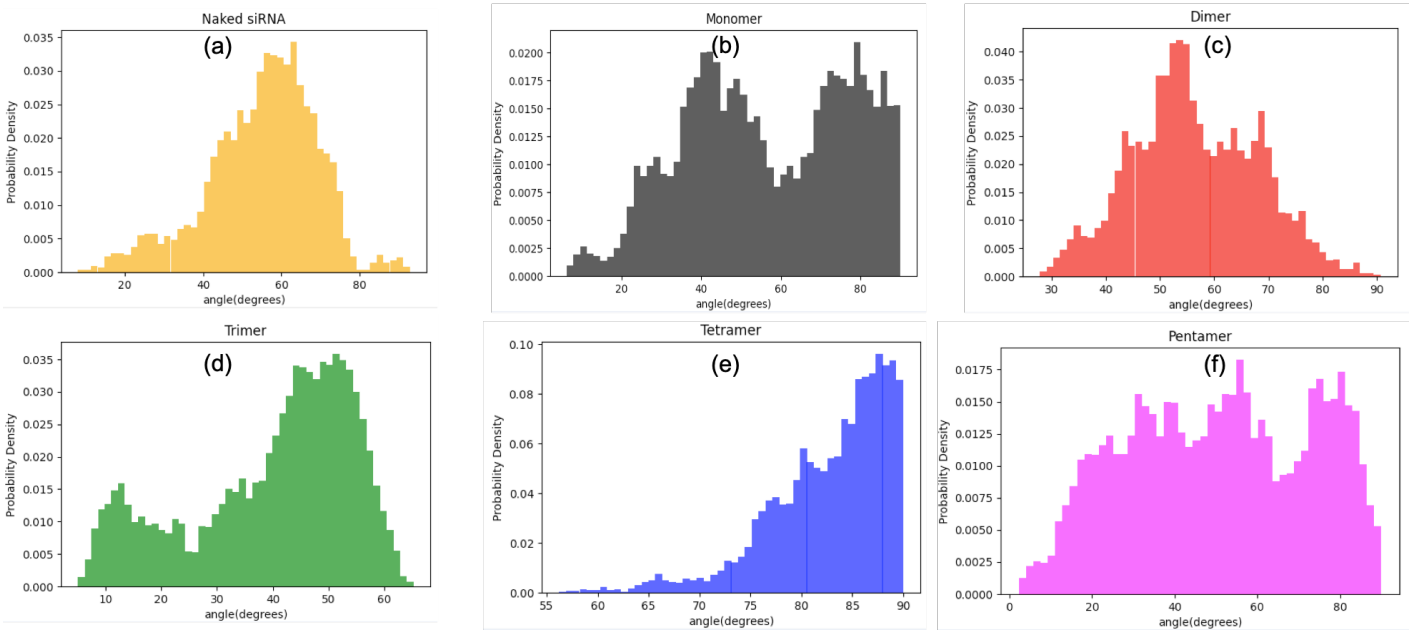

Fig. S5 Probability distributions of the siRNA tilt angle relative to membrane normal averaged over trajectories.

Fig.S3(b) and Fig.S5 collectively display the tilt angle and the most frequently observed orientation angle between the siRNA molecule and the membrane normal, monitored continuously throughout the unbiased molecular dynamics trajectories across various simulated systems. These analyses provide critical insight into the preferential orientational behavior adopted by naked siRNA and the different polyplex systems as they interact with the lipid bilayer surface. Notably, naked siRNA exhibits a characteristic tilt angle of approximately 60°, suggesting a moderately inclined orientation relative to the membrane normal, indicative of a partially tilted engagement with the membrane surface. In contrast, the majority of polyplex systems consistently demonstrate a dominant tilt angle of approximately 90° with respect to the membrane normal, signifying that the polyplexes preferentially orient themselves parallel to the membrane surface upon approach and interaction with the lipid bilayer. This pronounced orientational distinction between naked siRNA and the polyplex systems carries significant mechanistic implications. The tendency of polyplexes to land and reside parallel to the membrane surface is entirely consistent and well-aligned with the observations derived from the biased SMD simulations presented in Fig.S4, wherein the submarine configuration — characterized by the complex orienting perpendicular to the membrane normal — was identified as the dominant intermediate orientation during the membrane translocation process. Together, these complementary analyses from both unbiased and biased simulation frameworks coherently reinforce the conclusion that NAPA oligomer complexation fundamentally governs the orientational dynamics of siRNA at the membrane interface, potentially facilitating a more organized and favorable pathway for membrane translocation.

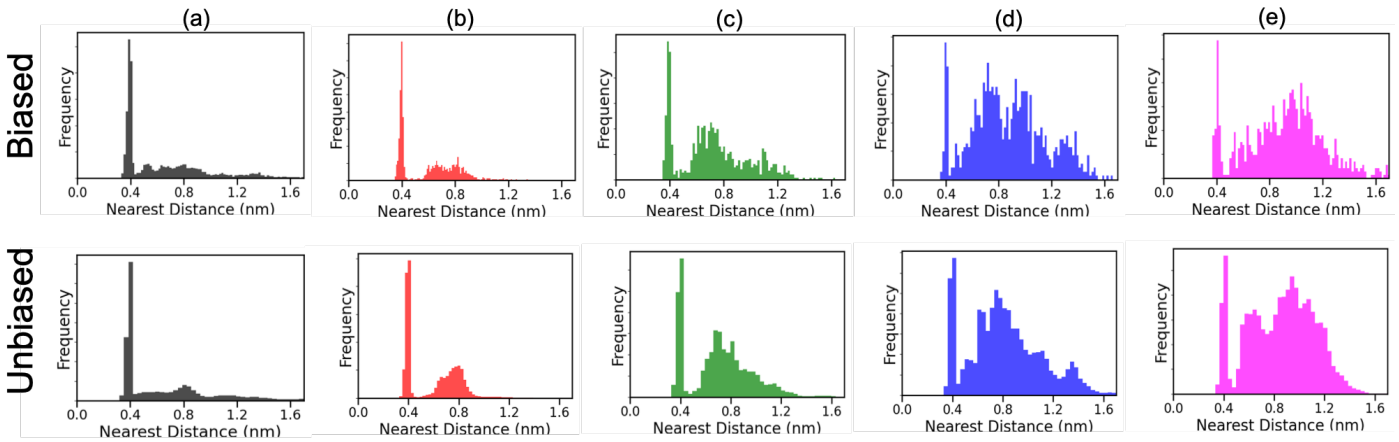

Fig. S6 Probability distribution of the closest phosphate atom of siRNA and the nitrogen atoms of (a) monomer, (b) dimer, (c) trimer, (d) tetramer, and (e) pentamer molecules during the biased and unbiased simulations.

0.1 Phosphate-Nitrogen distance distributions in polyplexes

Fig.S6 presents a comparative analysis of the distribution of distances measured from the nearest siRNA phosphate atom to the nitrogen atoms of various NAPA oligomers, evaluated across both biased and unbiased simulation frameworks, with the primary objective of elucidating the nature and extent of complexation between siRNA and the NAPA oligomers of varying chain lengths. Across all polyplex systems examined, oligomers consistently form close, stable contacts with the siRNA, with interaction distances ranging from 0.4 to 1.6 nm. This range of distances confirms electrostatic interactions between the positively charged nitrogen atoms of the NAPA oligomers and the negatively charged phosphate backbone of the siRNA, collectively validating complexation across all simulated polyplex configurations. A particularly informative trend emerges when comparing contact-distance distributions across oligomer sizes. Smaller oligomers, specifically in Fig.S6(a-b), the monomer and dimer, exhibit the majority of their interactions with siRNA within a relatively narrow and close proximity range of up to 0.9 nm, reflecting their structurally compact and geometrically simple nature, which allows them to engage tightly and directly with the siRNA phosphate backbone without significant steric hindrance. In contrast, Fig.S6(c-e) shows that the higher-order NAPA oligomers comprising the trimer, tetramer, and pentamer display interaction distances extending visibly up to 1.6 nm. This broader distribution of contact distances in larger NAPA oligomers can be attributed to their inherently more complex three-dimensional structures and diverse orientational configurations when wrapped around the siRNA molecule, introducing greater spatial heterogeneity in the positioning of their nitrogen atoms relative to the siRNA phosphate groups.

1 Equilibrium conformations of polyplexes from umbrella sampling simulations

Fig.S7(a-f) presents representative snapshots of six distinct system configurations, captured from the final frame of each 5 ns simulation window extracted from the umbrella sampling simulations, providing a comprehensive visual account of the membrane interaction behavior of naked siRNA and various polyplex systems under the applied biasing potential. As illustrated across the six panels, all six simulated systems successfully attach to the lipid membrane following the umbrella sampling procedure, confirming the ability of both naked siRNA and siRNA-NAPA oligomer complexes to establish stable membrane associations under the enhanced sampling conditions. Several key structural observations emerge from this analysis. First, both naked siRNA and the polyplex systems are consistently found to orient and land parallel to the membrane normal upon membrane attachment, corroborating the orientational trends previously identified in the unbiased trajectory analyses presented in Fig.S3(b) and Fig.S5, and further reinforcing the notion that this parallel orientation represents a thermodynamically preferred configuration at the membrane interface. Second, in the systems involving smaller oligomers, specifically the monomer, dimer, and trimer complexes, a notable dispersion of the respective oligomers into the surrounding aqueous solution is observed, suggesting that the binding affinity of these shorter chain oligomers to siRNA is comparatively weaker, allowing solvation of individual oligomer units during the course of the simulation. Finally, a structurally significant and visually prominent inward membrane bulge is observed in all systems upon attachment of the

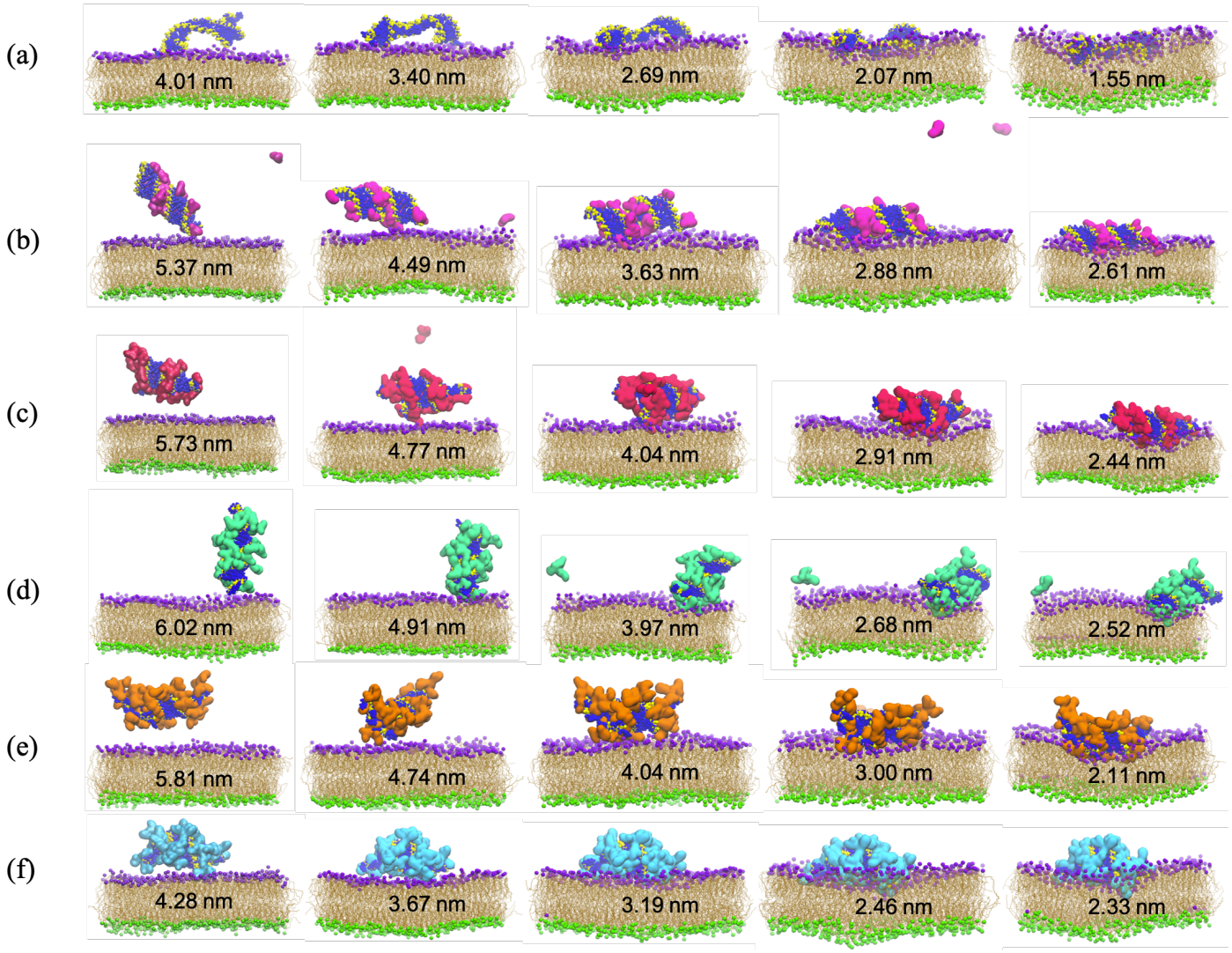

Fig. S7 Final conformational snapshots extracted from 5 ns umbrella sampling simulations for each system. Correspondingly, reaction coordinates are written for each system. Color code: as in Figure 1.

naked siRNA and polyplex complexes to the membrane surface. This pronounced membrane deformation reflects the substantial mechanical stress exerted on the lipid bilayer by electrostatic and steric interactions between the complexes and the membrane headgroups, highlighting the physical impact of polyplex attachment on membrane structural integrity.

References

1 S. Jo, T. Kim, V. G. Iyer and W. Im, *J. Comput. Chem.*, 2008, **29**, 1859–1865.

2 D. D. Yadav, D. Bhandary and P. Paik, *J. Phys. Chem. B*, 2025, **129**, 8166–8176.

3 M. J. Abraham, T. Murtola, R. Schulz, S. Páll, J. C. Smith, B. Hess and E. Lindahl, *SoftwareX*, 2015, **1-2**, 19–25.

4 T. Darden, D. York and L. Pedersen, *J. Chem. Phys.*, 1993, **98**, 10089–10092.

5 J. C. Dyre, *J. Chem. Phys.*, 2018, **149**, 210901.

6 A. Gray, *Modern Differential Geometry of Curves and Surfaces with Mathematica*, CRC Press, Boca Raton, FL, 2nd edn, 1997, pp. 398–401.